

University of Wollongong

## Research Online

---

Australian Institute for Innovative Materials -  
Papers

Australian Institute for Innovative Materials

---

2012

### Magnetocapacitance effect in nonmultiferroic YFeO<sub>3</sub> single crystal

Z X. Cheng

*University of Wollongong, cheng@uow.edu.au*

H Shen

*Shanghai Institute Of Technology*

J Xu

*Chinese Academy Of Sciences, Shanghai Institute Of Technology*

Peng Liu

*University of Wollongong, pl990@uowmail.edu.au*

S J. Zhang

*Pennsylvania State University*

*See next page for additional authors*

Follow this and additional works at: <https://ro.uow.edu.au/aiimpapers>



Part of the [Engineering Commons](#), and the [Physical Sciences and Mathematics Commons](#)

---

#### Recommended Citation

Cheng, Z X.; Shen, H; Xu, J; Liu, Peng; Zhang, S J.; Wang, Jianli; Wang, Xiaolin; and Dou, S X., "Magnetocapacitance effect in nonmultiferroic YFeO<sub>3</sub> single crystal" (2012). *Australian Institute for Innovative Materials - Papers*. 561.  
<https://ro.uow.edu.au/aiimpapers/561>

Research Online is the open access institutional repository for the University of Wollongong. For further information contact the UOW Library: [research-pubs@uow.edu.au](mailto:research-pubs@uow.edu.au)

---

## Magnetocapacitance effect in nonmultiferroic YFeO<sub>3</sub> single crystal

### Abstract

YFeO<sub>3</sub> single crystal displays two relaxor-like dielectric relaxations, one at low temperature (170300 K) and one at high temperature (370520 K), which are attributed to the activation of electrons and oxygen vacancies, respectively. Above the temperature at which electrons are activated, the sample displays a large magnetocapacitance effect. Comparison of the impedance Cole-Cole plots measured with and without applied magnetic field reveals that the occurrence of magnetocapacitance effect is accompanied with an increasing in DC conductivity under magnetic field after the activation of electrons, which is explained by the enhancement of electron jumping in Fe<sup>2+</sup>-O-Fe<sup>3+</sup> chains by magnetic field. Thus the magnetocapacitance effect in YFeO<sub>3</sub> single crystal can be explained by the combination of the Maxwell-Wagner space charge effect and/or magnetoresistance effect, depending on the frequency range.

### Keywords

effect, single, crystal, nonmultiferroic, magnetocapacitance, yfe03

### Disciplines

Engineering | Physical Sciences and Mathematics

### Publication Details

Cheng, Z. X., Shen, H., Xu, J., Liu, P., Zhang, S. J., Wang, J. L., Wang, X. L. & Dou, S. X. (2012). Magnetocapacitance effect in nonmultiferroic YFeO<sub>3</sub> single crystal. *Journal of Applied Physics*, 111 (3), 034103-1-034103-5.

### Authors

Z X. Cheng, H Shen, J Xu, Peng Liu, S J. Zhang, Jianli Wang, Xiaolin Wang, and S X. Dou

## Magnetocapacitance effect in nonmultiferroic YFeO<sub>3</sub> single crystal

Z. X. Cheng, H. Shen, J. Y. Xu, P. Liu, S. J. Zhang et al.

Citation: *J. Appl. Phys.* **111**, 034103 (2012); doi: 10.1063/1.3681294

View online: <http://dx.doi.org/10.1063/1.3681294>

View Table of Contents: <http://jap.aip.org/resource/1/JAPIAU/v111/i3>

Published by the American Institute of Physics.

---

### Related Articles

Role of deep and shallow donor levels on n-type conductivity of hydrothermal ZnO

*Appl. Phys. Lett.* **100**, 052115 (2012)

High-field linear magneto-resistance in topological insulator Bi<sub>2</sub>Se<sub>3</sub> thin films

*Appl. Phys. Lett.* **100**, 032105 (2012)

Anisotropic electrical transport properties of poly(methyl methacrylate) infiltrated aligned carbon nanotube mats

*Appl. Phys. Lett.* **100**, 022108 (2012)

Magnetoresistance oscillations arising from edge-localized electrons in low-defect graphene antidot-lattices

*Appl. Phys. Lett.* **100**, 023104 (2012)

Correlation between the ferromagnetic metal percolation and the sign evolution of angular dependent magnetoresistance in Pr<sub>0.7</sub>Ca<sub>0.3</sub>MnO<sub>3</sub> film

*Appl. Phys. Lett.* **99**, 252502 (2011)

---

### Additional information on J. Appl. Phys.

Journal Homepage: <http://jap.aip.org/>

Journal Information: [http://jap.aip.org/about/about\\_the\\_journal](http://jap.aip.org/about/about_the_journal)

Top downloads: [http://jap.aip.org/features/most\\_downloaded](http://jap.aip.org/features/most_downloaded)

Information for Authors: <http://jap.aip.org/authors>

## ADVERTISEMENT



# Magnetocapacitance effect in nonmultiferroic $\text{YFeO}_3$ single crystal

Z. X. Cheng,<sup>1,a)</sup> H. Shen,<sup>2</sup> J. Y. Xu,<sup>2</sup> P. Liu,<sup>1</sup> S. J. Zhang,<sup>3</sup> J. L. Wang,<sup>1</sup> X. L. Wang,<sup>1</sup> and S. X. Dou<sup>1</sup>

<sup>1</sup>*Institute for Superconducting and Electronic Materials, University of Wollongong, NSW 2519, Australia*

<sup>2</sup>*Shanghai Institute of Technology, Shanghai, China*

<sup>3</sup>*Materials Research Institute, Pennsylvania State University, Pennsylvania 16802, USA*

(Received 28 August 2011; accepted 5 January 2012; published online 3 February 2012)

$\text{YFeO}_3$  single crystal displays two relaxor-like dielectric relaxations, one at low temperature (170–300 K) and one at high temperature (370–520 K), which are attributed to the activation of electrons and oxygen vacancies, respectively. Above the temperature at which electrons are activated, the sample displays a large magnetocapacitance effect. Comparison of the impedance Cole-Cole plots measured with and without applied magnetic field reveals that the occurrence of magnetocapacitance effect is accompanied with an increasing in DC conductivity under magnetic field after the activation of electrons, which is explained by the enhancement of electron jumping in  $\text{Fe}^{2+}\text{-O-Fe}^{3+}$  chains by magnetic field. Thus the magnetocapacitance effect in  $\text{YFeO}_3$  single crystal can be explained by the combination of the Maxwell-Wagner space charge effect and/or magnetoresistance effect, depending on the frequency range. © 2012 American Institute of Physics. [doi:10.1063/1.3681294]

## I. INTRODUCTION

In recent years, the search for the magnetoelectric (ME) coupling effect has been an important focus of research, due to the great potential for application in multistate memories and sensors.<sup>1–4</sup> Generally, to display the ME effect, the material candidate needs to be magnetic (ferromagnetic or antiferromagnetic). Therefore, many candidates are from the class of materials containing magnetic transition metal ions. Due to variable valences caused by dislocations and oxygen deficiencies, which can usually act as charge carriers, these materials are quite conductive. Therefore many observed ME materials may not be intrinsic, from magnetoelectric coupling, but extrinsic, from changing resistivity under magnetic field. The Maxwell-Wagner space charge effect at the interface of sample and electrode or grain boundaries can result in artificial dielectric relaxation,<sup>5</sup> and its combination with magnetoresistance (MR) can create a magnetocapacitance effect, even in a nonmultiferroic material without magnetoelectric coupling, as theoretically predicted by Catalan.<sup>6</sup> Therefore, for this particular case of an ME effect in nonmultiferroic materials, a change in the resistivity of the material in magnetic field through an intrinsic MR effect from double-exchange or spin-polarized tunneling across grain boundaries is crucial for the observation of the ME effect. However, there is a lack of experimental data to detect the ME effect where the MR effect of the material is simultaneously examined.  $\text{YFeO}_3$ , crystallizing in an orthorhombic perovskite structure and displaying weak ferromagnetism below its Néel temperature ( $T_N = 640$  K), is a nonferroelectric material.<sup>7–13</sup> In this letter, a large positive magnetocapacitance effect is observed in  $\text{YFeO}_3$  single crystal. Through

analysis of the complex impedance spectra, the direct cause for the magnetocapacitance was proposed.

## II. EXPERIMENT DETAILS

The  $\text{YFeO}_3$  single crystal used in this work was grown by the floating zone method. A mixture of  $\text{Y}_2\text{O}_3$  (99.99%) and  $\text{Fe}_2\text{O}_3$  (99.99%) powders with a stoichiometric ratio composition was used as the starting material for the single crystal growth. Polycrystalline rods were fabricated after double sintering at 1100 °C and 1550 °C, with intermediate crushing and grinding, and these were used as feed and seed rods for single crystal growth. A floating zone furnace equipped with two ellipsoidal mirrors was employed for the single crystal growth, using two 3.5 kW halogen lamps as heat sources. The feed and seed shafts rotated at 5–20 rpm in opposite directions, and the crystal was grown from the bottom to the top in a vertical direction. The traveling rate of the melting zone was in the range of 2.5–7.5 mm/h in 1 bar of oxygen. The crystal structures of the samples were examined by x-ray diffraction (XRD), using Cu-K $\alpha$  radiation at  $\lambda = 1.54056$  Å. Rietveld refinement calculations were conducted via the Rietica software package based on the observed XRD pattern. Iron valence states were identified by x-ray photoelectron spectrometry (XPS) and Mössbauer spectra. Magnetic property measurements of the samples were conducted on a Quantum Design magnetic properties measurement system (MPMS) and a 14 T physical properties measurement system (PPMS) equipped with a vibrating sample magnetometer (VSM). For the dielectric tests, a (100) wafer with dimensions of  $4 \times 3 \times 1$  mm<sup>3</sup> was coated on both sides with silver paste as electrodes. Measurements were carried out on an Agilent 4284a LCR meter. Dielectric and impedance measurement in magnetic field is carried out using a combination of an Agilent 4294a impedance analyzer and a PPMS.

<sup>a)</sup>Author to whom correspondence should be addressed. Electronic mail: cheng@uow.edu.au.

### III. RESULTS AND DISCUSSION

Figure 1 shows the XRD pattern of the  $\text{YFeO}_3$  powder obtained from grinding a piece cut from a crack-free single crystal. A good refinement with goodness of refinement ( $R_p$ ) of 7.1 can be obtained using an orthorhombic perovskite structure with space group  $Pnma$ . The obtained lattice parameters are  $a = 5.5961$ ,  $b = 7.6029$ , and  $c = 5.2801$  Å. For comparison, the values of lattice parameters of the standard, PDF 01-086-0171, are  $a = 5.5877$ ,  $b = 7.5951$ , and  $c = 5.2743$  Å, with the lattice extending in three directions. To further check the quality of the single crystal, the crystal was oriented and a (100) wafer was cut and polished. A mirror-like surface was obtained without any cracks observable by optical microscope. The x-ray rocking curve of the crystal wafer examined by high resolution XRD shows that the profile of (200) diffraction has a symmetrical peak, with a full-width at half-maximum (FWHM) of 24 arc sec (shown as the inset of Fig. 1). The nearly perfect shape without any shoulder confirms the absence of any subgrains, indicating the excellent quality of the crystal.

Figure 2(a) shows the Fe 2*p* XPS spectrum of the  $\text{YFeO}_3$  crystal. Usually, the  $\text{Fe}^{3+} 2p_{3/2}$  line is at about 711.5 eV and associated with a satellite peak 8 eV above this principal peak, while  $\text{Fe}^{2+}$  displays a principal peak at around 709.5 eV and has a satellite peak 6 eV above it.<sup>14</sup> Gaussian-Lorentzian curve fitting shows that the Fe 2*p*<sub>3/2</sub> peak in the  $\text{YFeO}_3$  single crystal sample can be separated into two peaks. The total amount of  $\text{Fe}^{2+}$  ions is estimated to be less than 5% of the total number of Fe ions. The presence of the  $\text{Fe}^{2+}$  is attributed to oxygen vacancies, which are very common in perovskite compounds. The content of  $\text{Fe}^{2+}$  is further confirmed by Mössbauer spectra at 300 K, which has been fitted by two subspectra: one sextet (97%) and one doublet (3%). This indicates that the content of  $\text{Fe}^{2+}$  in our  $\text{YFeO}_3$  single crystal is 3% [shown in Fig. 2(b)].

Figure 3 shows the zero field cooled (ZFC) magnetization of  $\text{YFeO}_3$  in magnetic field of 100 Oe, and both the zero-field cooled and field cooled (FC) magnetization in 1 T, from 310 to 750 K. Based on the magnetization curves, the sample experiences a ferromagnetic-like transition at a tem-

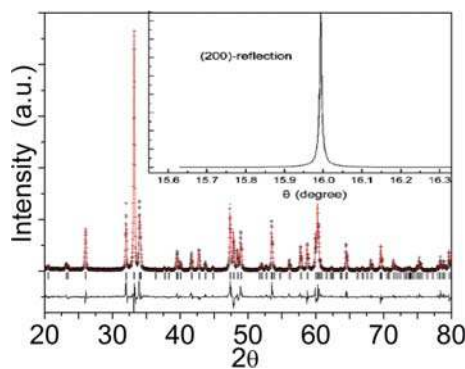


FIG. 1. (Color online) XRD observed (+) and calculated (—) profile, and difference profile (bottom trace) for  $\text{YFeO}_3$  single crystal at room temperature. The bars indicate the diffraction peak positions in the standard. Inset is the profile of the high resolution diffraction peak of the (100) oriented wafer.

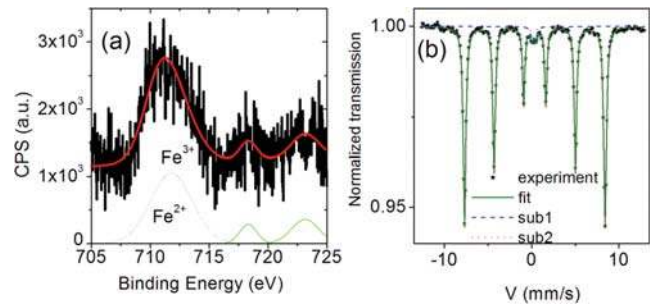


FIG. 2. (Color online) (a) XPS spectrum of Fe 2*p* peaks in  $\text{YFeO}_3$  crystal. (b) Mössbauer spectra of  $\text{YFeO}_3$  at 300 K.

perature of around 640 K, which is a typical canted antiferromagnetic transition due to the very small magnetic moment displayed by the sample. To determine the transition temperature, a thermoremanent magnetization measurement (TRM) was carried out, which showed a magnetic transition at exactly 640 K. This temperature is very close to the transition temperature obtained from specific heat measurements on the same single crystal sample. For FC and ZFC  $M$ - $T$  curves measured in the low temperature range from 10 to 310 K (not shown here), no obvious magnetic transition was observed. Using the linear Curie-Weiss law fitting of the  $M$ - $T$  curve in the paramagnetic state of the sample from 700 to 750 K, a  $\mu_{\text{eff}}$  of  $6.5 \mu_B$  is obtained (shown as the upper left inset of Fig. 3). Therefore  $\text{Fe}^{3+}$  in  $\text{YFeO}_3$  is in the high spin state ( $HS$ ) with an electron configuration of  $t_{2g}^3 e_g^2$ , if the very tiny amount of  $\text{Fe}^{2+}$  is not taken into account here. A negative Curie Weiss temperature of  $\Theta = -1256$  K was obtained by linear fitting, indicating that a very strong antiferromagnetic ordering must have occurred below this paramagnetic temperature. The nearest-neighbor exchange integral  $J$  was estimated using the Curie Weiss temperature,  $\theta_{\text{CW}} = -1/3 qJS(S+1)$ , where  $S$  is the spin number of  $\text{Fe}^{3+}$ , which is  $5/2$ , and  $q$  is the number of nearest neighbor magnetic ions, which is 6 for  $\text{YFeO}_3$ . The exchange integral  $J$  is thus obtained as 6.2 meV. Magnetization versus magnetic field ( $M$ - $H$ ) curves of  $\text{YFeO}_3$  single crystal were collected at 645 and 635 K, which are temperatures above and below  $T_N$ , as shown in the upper right inset of Fig. 3. The

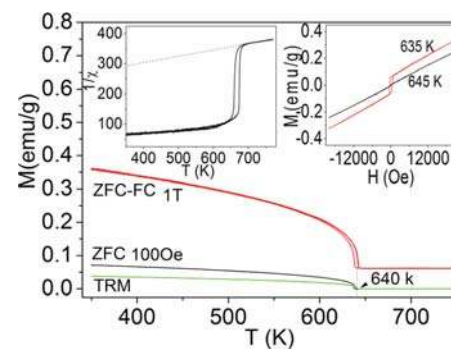


FIG. 3. (Color online) Temperature dependence of the magnetization of  $\text{YFeO}_3$  in fields of 100 Oe and 1 T, and for a thermoremanent magnetization measurement, measured from 310 K to 750 K. Left inset is the Curie-Weiss law fitting for temperatures from 700 to 750 K. Right inset is magnetization vs magnetic field measured at 635 K (below  $T_N$ ) and 645 K (above  $T_N$ ).



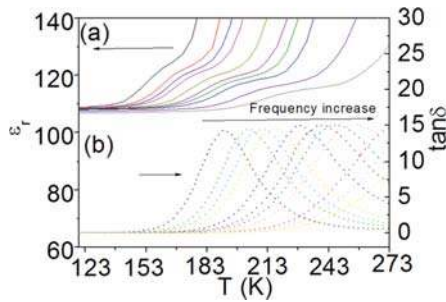


FIG. 4. (Color online) Temperature dependence of the dielectric constant (a) and loss tangent (b) from 1 kHz to 1 MHz in the temperature range from 100 to 300 K.

$M$ - $H$  curve is a straight line at 645 K, which corresponds to the paramagnetic state of the sample at this temperature. At 635 K, the curve displays obvious hysteretic behavior, with a dominant linear contribution. The rectangular hysteresis loop displays a coercive field of 400 Oe and remanent magnetization of 0.055 emu/g.  $\text{YFeO}_3$  is a canted antiferromagnet due to the 180 deg bonding interaction of  $\text{Fe}^{3+}$ -O- $\text{Fe}^{3+}$ , and thus exhibits weak ferromagnetic behavior.

Results of dielectric measurements at low temperature are shown in Fig. 4. It can be seen that both the relative dielectric constant ( $\epsilon_r$ ) and the loss tangent ( $\tan \delta$ ) become frequency and temperature independent at temperatures lower than 140 K. In this temperature range, the static dielectric constant  $\epsilon_s$  and the high-frequency limit dielectric constant  $\epsilon_\infty$  reach a common limit value of  $\sim 100$ . With temperature increasing, in the temperature range of 170–300 K, the dielectric constant shows a sharp increase and then reaches a plateau. The inflection temperature for the dielectric constant shifts to higher temperature with increasing frequency, indicating relaxor-like dielectric behavior. A broad dielectric loss peak occurs, corresponding to the abnormal dielectric relaxation. The loss peak also shifts to higher temperatures with increasing frequency, which indicates a thermally activated relaxation process. The dielectric loss increases a little with further increasing temperature, which is ascribed to the contribution of DC conductivity in the single crystal. With the temperature increasing even further, in high temperatures from 370 to 520 K, another relaxor-like abnormal dielectric peak was observed (as shown in Fig. 5(b)). Above this temperature,  $\text{YMnO}_3$  will experience a transition from semiconductor-like to metallic and, correspond-

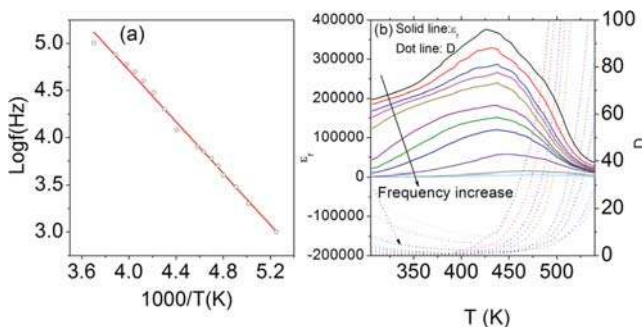


FIG. 5. (Color online) (a) is the Arrhenius plot for the low-temperature relaxation, with the solid line indicating the least squares linear fitting; (b) shows the dielectric behavior in the high temperature range.

ingly, dielectric constant will decrease and finally display a negative value. Both the low and the high temperature dielectric relaxations can be described by the modified Debye theory.<sup>15</sup> According to the Debye theory, the thermal dielectric activation can be approximately determined by the dielectric loss ( $\tan \delta$ ) measurement and is described by the Arrhenius relationship,  $f = f_0 \exp(-U/k_B T)$ , where  $f$  is the characteristic frequency ( $f = 1/2\pi\tau$ ,  $\tau$  is the relaxation time),  $k_B T$  is the thermal energy,  $f_0$  is a prefactor and  $U$  is the activation energy. Figure 5(a) shows the Arrhenius plot of the log of the frequency versus  $1/T$ , and least-mean-squares analysis yields  $f_0 = 1 \times 10^{10.2}$  Hz and an activation energy of  $U = 0.12$  eV, which are typical values for electron type activation. It has been shown that Maxwell-Wagner-type contribution of depletion layers at the interface between sample and contacts can result in such kind of broad dielectric relaxation. Therefore it is very likely that the dielectric relaxation at low temperature range is due to Maxwell-Wagner space charge effect. Another possible reason for the low temperature dielectric relaxation is the activation of electrons at  $\text{Fe}^{2+}/\text{Fe}^{3+}$  sites. XPS and Mössbauer spectra show that there is a tiny amount of  $\text{Fe}^{2+}$  in the  $\text{YFeO}_3$  crystal. Each  $\text{Fe}^{2+}$  with its surrounding  $\text{Fe}^{3+}$  will form a dipole with strong local polarization. Under an external electric field, the hopping of electrons between  $\text{Fe}^{2+}$  and  $\text{Fe}^{3+}$ , which is equivalent to the reversal of the dipole, contributes to the large dielectric constant, as suggested in a ceramic sample and a  $\text{LuFe}_2\text{O}_4$  sample.<sup>16–18</sup> Therefore the activation of space charges here will include contribution both from Maxwell-Wagner space charge of depletion layers at the interface between sample and contacts, and electrons in the  $\text{Fe}^{2+}/\text{Fe}^{3+}$  dipoles. For the dielectric relaxation in the high temperature range of 370–520 K, the dielectric loss peak cannot be identified due to the huge values. Through high temperature DC resistance measurements, an activation energy of 1.10 eV is obtained. This value reflects a typical thermal activation process involving oxygen vacancies.<sup>19,20</sup> The presence of oxygen vacancies is in accordance with the presence of a small amount of  $\text{Fe}^{2+}$ , as confirmed by the XPS and Mössbauer spectra.

The magnetic field effect on the sample capacitance was measured under different magnetic fields at the three temperatures of 70, 220, and 305 K (shown in Fig. 6). The

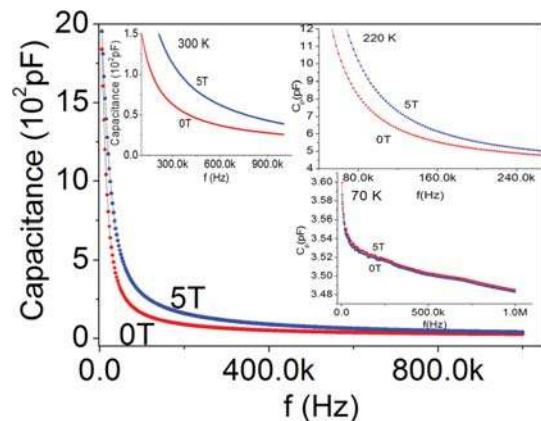


FIG. 6. (Color online) Capacitance of  $\text{YFeO}_3$  single crystal capacitor measured in zero field and 5 T field, at temperatures of 305 (magnified high frequency part is also shown), 70, and 220 K.

capacitance of the sample displays a variety of dependencies on magnetic field over a wide frequency range at different temperatures. At 70 K, the magnetic field has little effect on the dielectric response of the sample. At 220 K, above the temperature for the low temperature dielectric relaxation, the capacitance of the sample is enhanced by application of magnetic field, and the increase is more obvious in the low frequency range than in the high frequency range, up to 34% at 50 kHz in a 5 T field and 1% at 900 kHz in the same field. At 305 K, the magnitude of the enhancement is further increased to 74% at 50 kHz in a 5 T magnetic field, and 60% at 900 kHz in the same magnetic field.

In order to clarify the observed magnetocapacitance effect, impedance spectroscopy of the  $\text{YFeO}_3$  single crystal was conducted at different temperatures with and without magnetic field, and the results are presented in the form of Cole-Cole plots (shown in Fig. 7). It can be seen that the impedance Cole-Cole plot at 70 K is just a small part of a semicircle, which indicates that the sample at this temperature has very large static resistance. Furthermore, magnetic field has little effect on the Cole-Cole plot at this temperature. At 220 K, the impedance Cole-Cole plot changes significantly, displaying part of a semicircle and a linear rising tail at the lowest frequencies, which means a large decrease in the  $\text{YFeO}_3$  static resistance (the  $Z'$  value of the circle's intersection with the  $Z'$ -axis at the  $f=0$  Hz end) and a significant contribution from the electronic conductivity.<sup>21</sup> However, at this temperature, the magnetic field has a very apparent effect on the impedance behavior of  $\text{YFeO}_3$ , and a significant decrease in static impedance due to the magnetic field is observed. At 305 K, static impedance of the sample is further decreased, and a similar effect of magnetic field on static impedance was observed. Therefore, the observed large magnetocapacitance effect in the  $\text{YFeO}_3$  single crystal sample is accompanied by a significant decrease in static impedance or resistance in magnetic field, i.e., there is a significant increase in the conductivity of the sample. It is obvious that the magnetocapacitance effect is related to the activation of electrons, because no such effect was observed at 70 K, which is below the electron activation temperature of above 170 K. At temperatures below the low temperature dielectric

relaxation, all the 3d electrons of  $\text{Fe}^{2+}$  are localized at the  $\text{Fe}^{2+}$  positions, and  $\text{Fe}^{2+}/\text{Fe}^{3+}$  dipoles cannot follow the external electrical field variations. Above the temperature where the low temperature dielectric relaxation occurs, the electrons are activated, and switching of  $\text{Fe}^{2+}/\text{Fe}^{3+}$  dipoles, which occurs by jumping of electrons between  $\text{Fe}^{2+}$  and  $\text{Fe}^{3+}$ , become possible. The jumping of electrons from  $\text{Fe}^{2+}$  to  $\text{Fe}^{3+}$  will be via the intermediate O in  $\text{Fe}^{2+}\text{-O-Fe}^{3+}$  chains. Such an electron jumping process will follow the double exchange mechanism, in which the magnitude of the transfer process depends on the angle between the  $\text{Fe}^{2+}$  and the  $\text{Fe}^{3+}$  spins.<sup>22–24</sup> The possibility of electron jumping in  $\text{Fe}^{2+}\text{-O-Fe}^{3+}$  chains will not only increase the electronic conductivity of the sample, leading to a magnetoresistance effect because it follows from the double exchange mechanism of electron transfer, but also contribute the dielectric relaxation as the electrons jumping in  $\text{Fe}^{2+}/\text{Fe}^{3+}$  chains is also a dipole switching process. The observed increase in DC conductivity in  $\text{YFeO}_3$  single crystal in magnetic field at the temperature where electrons are activated is a good reflection of the above speculation. Furthermore, at 200 K, electrons are activated at 50 kHz while not activated at 900 kHz, therefore the increase of capacitance in magnetic field for low frequency range is larger than that for high frequency range. The activation of the electrons at low temperature range includes the activation of both electrons at the electrode/sample interface and electrons located at  $\text{Fe}^{2+}/\text{Fe}^{3+}$  dipoles. However, the electrons located at the electrode/sample interface have a response frequency below  $10^4$  Hz,<sup>5</sup> only electrons located at  $\text{Fe}^{2+}/\text{Fe}^{3+}$  dipoles have contribution to the magnetocapacitance effect at high frequency (for example, 900 kHz). This is the reason for the smaller magnetocapacitance observed at 300 K for 900 kHz in comparison to the larger value at lower frequency. Furthermore, the close values of magnetocapacitance effect at 900 and 50 kHz in magnetic field means the dominating contribution to magnetocapacitance effect is from electrons located at  $\text{Fe}^{2+}/\text{Fe}^{3+}$  dipoles.

#### IV. SUMMARY

The magnetocapacitance effect is observed in a nonmultiferroic material,  $\text{YFeO}_3$  single crystal. The activation of electrons in  $\text{Fe}^{2+}/\text{Fe}^{3+}$  dipoles in  $\text{YFeO}_3$  single crystal at low temperature contributes to the DC conductivity or MR effect in magnetic field due to the jumping of electrons following a double exchange mechanism. The combination of Maxwell-Magner space charge effect and MR effect result in a magnetocapacitance effect at low frequency range. Furthermore, the jumping of electrons in  $\text{Fe}^{2+}/\text{Fe}^{3+}$  dipoles is also a switching process of the dipole, which contributes to magnetocapacitance effect due to the jumping getting easier in magnetic field. The contribution from  $\text{Fe}^{2+}/\text{Fe}^{3+}$  dipoles switching dominated the magnetocapacitance effect at high frequency range (900 kHz). Although this ME effect in  $\text{YFeO}_3$  is not intrinsic, it still might be favorable for application, as more candidate materials can be obtained. This observation provides further evidence that large magnetoelectric coupling does not necessarily need multiferroic materials, and the origin of magnetoelectric coupling is quite diverse.<sup>25</sup>

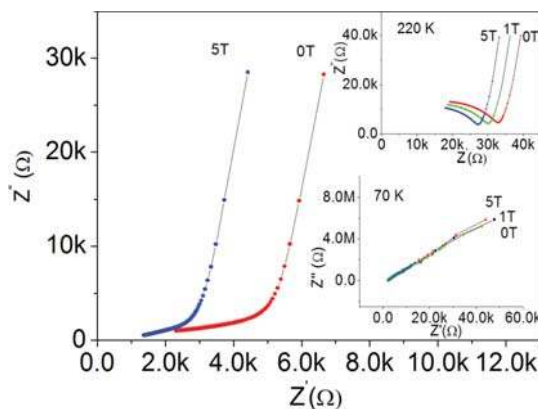


FIG. 7. (Color online) Impedance Cole-Cole plots in zero field and 5 T field of  $\text{YFeO}_3$  single crystal, measured at temperatures of 305, 70, and 220 K. 1 T plots are also shown in the insets.

## ACKNOWLEDGMENTS

Z. X. Cheng thanks the Australian Research Council for supporting this work through a Future Fellowship. H. Shen and J. Y. Xu thank the Natural Science Foundation of China for support (No. 51002097). We also thank Dr. Tania Silver for careful reading of this paper.

- <sup>1</sup>B. Ramesh and N. A. Spaldin, *Nature Mater.* **6**, 21 (2007).
- <sup>2</sup>M. Fiebig, *J. Phys. D* **38**, R123 (2005).
- <sup>3</sup>Z. X. Cheng, X. L. Wang, S. X. Dou, K. Ozawa, and H. Kimura, *Phys. Rev. B* **77**, 092101 (2008).
- <sup>4</sup>P. Liu, Z. X. Cheng, Y. Du, and X. L. Wang, *J. Phys. D* **43**, 325002 (2010).
- <sup>5</sup>N. Ortega, Ashok Kumar, R. S. Katiyar, and J. F. Scott, *Appl. Phys. Lett.* **91**, 102902 (2007).
- <sup>6</sup>G. Catalan, *Appl. Phys. Lett.* **88**, 102902 (2006).
- <sup>7</sup>Y. S. Didosyan, H. Hauser, J. Nicolics, and F. Haberl, *J. Appl. Phys.* **87**, 7079 (2000).
- <sup>8</sup>Y. S. Didosyan, H. Hauser, W. Fiala, J. Nicolics, and W. Toriser, *J. Appl. Phys.* **91**, 7000 (2002).
- <sup>9</sup>Y. S. Didosyan, H. Hauser, G. A. Raider, and W. Toriser, *J. Appl. Phys.* **95**, 7339 (2004).
- <sup>10</sup>Y. S. Didosyan, H. Hauser, and J. Nicolics, *Sens. Actuators, A* **81**, 263 (2000).
- <sup>11</sup>A. V. Kimel, A. Kirilyuk, A. Tsvetkov, R. V. Pisarev, and Th. Rasing, *Nature* **429**, 850 (2004).
- <sup>12</sup>H. Shen, J. Xu, A. Wu, J. Zhao, and M. Shi, *Mater. Sci. Eng., B* **157**, 77 (2009).
- <sup>13</sup>D. Treves, *J. Appl. Phys.* **36**, 1033 (1965).
- <sup>14</sup>C. Wandelt, *Surf. Sci. Rep.* **2**, 1 (1982).
- <sup>15</sup>K. S. Cole and R. H. Cole, *J. Chem. Phys.* **9**, 341 (1941).
- <sup>16</sup>P. Lunkenheimer, V. Bobnar, A. V. Pronin, A. I. Ritus, A. A. Volkow, and A. Loidl, *Phys. Rev. B* **66**, 052105 (2002).
- <sup>17</sup>Y. Ma, X. M. Chen, and Y. Q. Lin, *J. Appl. Phys.* **103**, 124111 (2008).
- <sup>18</sup>N. Ikeda, H. Ohsumi, K. Ohwada, K. Ishii, T. Inami, K. Kakurai, Y. Murakami, Y. Yoshii, S. Mori, Y. Horibe, and H. Kito, *Nature* **436**, 1136 (2005).
- <sup>19</sup>S. A. Hayward, F. D. Morrison, S. A. T. Redfern, E. K. H. Salje, J. F. Scott, K. S. Knight, S. Tarantino, A. M. Glazer, V. Shuvaeva, P. Daniel, M. Zhang, and M. A. Carpenter, *Phys. Rev. B* **72**, 054110 (2005).
- <sup>20</sup>M. Dawber, J. F. Scott, and A. J. Hartmann, *J. Eur. Ceram. Soc.* **21**, 1633 (2001).
- <sup>21</sup>A. K. Jonscher, *Dielectric Relaxation in Solids* (Chelsea Dielectrics Press, London, 1983).
- <sup>22</sup>C. Zener, *Phys. Rev.* **82**, 403 (1951).
- <sup>23</sup>G. Catalan and J. F. Scott, *Adv. Mater.* **21**, 2463 (2009).
- <sup>24</sup>W. Eerenstein, N. D. Mathur, and J. F. Scott, *Nature* **442**, 759 (2006).
- <sup>25</sup>J. F. Scott, *J. Magn. Magn. Mater.* **321**, 1689 (2009).